JOURNAL OF GEOPHYSICAL RESEARCH, VOL. 106, NO. D19, PAGES 22,647–22,653, OCTOBER 16, 2001

Polarization of the moonlit clear night sky measured by full-sky imaging polarimetry at full Moon: Comparison of the polarization of moonlit and sunlit skies

József Gál, Gábor Horváth , and András Barta

Department of Biological Physics, Eötvös University, Budapest, Hungary

Rüdiger Wehner

Zoologisches Institut, Universität Zürich, Zürich, Switzerland

Abstract. Using 180° field of view (full-sky) imaging polarimetry, the patterns of the degree and angle of polarization of the moonlit clear night sky were measured in every half an hour throughout the night at full Moon. The patterns were compared with those of the sunlit sky. The observed patterns including the positions of the Arago and Babinet neutral points of the moonlit night sky and sunlit day sky are practically identical if the zenith angle of the Moon is the same as that of the sun. The possible biological relevance of the polarization pattern of the moonlit night sky in the polarization vision and orientation of night-active insects is briefly discussed.

1. Introduction

The light of the night sky originates from the following main natural sources (in order of brightness): moonlight, stars and planets, the Milky Way, zodiacal light, airglow, and the light from these sources scattered by the Earth's atmosphere. Unfortunately, light pollution from artificial (city) lighting also affects many sites' night skies. Most of these sources are weakly polarized; the airglow is unpolarized [*Wolstencroft and Brandt*, 1974]; and the skylight may be strongly polarized [*Können*, 1985]. In the polarimetry of the night sky the unpolarized airglow emission and the atmospheric scattering of light of bright sources (e.g., the Moon) are unwanted because the former causes a dilution of the degree of polarization and the latter (the so-called "sky foreground") introduces a spurious polarization. The flux of these unwanted sources can be brighter than the source of interest, depending on direction and wavelength. At full Moon, in extended regions of the sky around the Moon and anti-Moon, the moonlight scattered and polarized in the atmosphere overwhelms all other sources of the night sky. This makes astronomical measurement more difficult; thus usually one must wait for a moonless night to make delicate polarimetric measurements.

Although in the last decades several extensive polarimetric investigations of the night sky were carried out [e.g., *Gehrels*, 1974], not much attention has been paid to the polarization characteristics of the moonlit night sky. The reason for this is clear: The main polarization characteristics (magnitude and distribution of the degree and angle of polarization) of the moonlit night sky should be the same as that of the normal daytime sky. Although few surprises are to be expected, we decided to check the similarities between moonlit and sunlit sky polarization experimentally.

Because of the difficulty of the measurement of the distribution of polarization over the moonlit night sky as well as to the expected similarity of the polarization characteristics of the moonlit sky to that of the sunlit sky, until now noone measured the polarization distribution of the moonlit sky. The aim of this work is to fill this gap and to obtain full-sky imaging polarimetric data of the moonlit clear night sky. Using 180° field of view imaging polarimetry, we measured the patterns of the degree and angle of polarization of the entire clear night sky at full Moon for different zenith angles of the Moon. These patterns were compared with the corresponding polarization patterns of the sunlit clear day sky measured with the same technique. The characteristics of the lunar neutral points of skylight polarization observed at full Moon were also compared with those of the corresponding Arago and Babinet neutral points of the sunlit sky. The polarization pattern of the moonlit night sky may possess also a biological significance in the polarization vision and orientation of nocturnal insects, which is also briefly discussed.

2. Materials and Methods

2.1. Places and Times of the Polarimetric Measurements

Our moonlight polarization measurements were performed in southern Hungary, in the immediate vicin-

Paper number 2000JD000085.
0148-0227/01/2000JD000085$09.00

Table 1. Recording Data of the Polarization Patterns of the Clear Moonlit Night Sky in Figures 2a-2c Measured by Full-Sky Imaging Polarimetry on May 17-18, 2000, in Kunfehértó (Hungary, 46°23'N, 19°24'E)*

	Row in Figures 2a-2c								
	1	2	3	4	5	6	7	8	9
Day May 2000	17	17	17	18	18	18	18	18	18
Time, UTC+2 local summer time	2235	2305	2334	0005	0035	0105	0135	0210	0250
Lunar zenith angle θ_M	70°	68°	64°	63°	63°	63°	64°	67°	70°
Lunar azimuth angle φ	142°	149°	155°	163°	172°	180°	187°	196°	204°

* The lunar azimuth angle φ is measured anticlockwise from north.

ity of the village Kunfehértó (46°23'N, 19°24'E; bright sandy and grassy terrain with a small alkaline lake, the diameter of which is $\sim$ 300 m, and the surface of which was flat during our measurements due to calmness at night) on May 17 and 18, 2000, at approximately full Moon (phase angle of the Moon was 9°4') when the sky was clear throughout the night. At full Moon (when the phase angle of the Moon is 0°) the moonlight is unpolarized; otherwise, it is slightly linear polarized with $p < 8.7\%$ [*Dollfus*, 1961; *Pellicori*, 1971]. At the place of our measurements the local summer time (UTC+2) of moonrise, culmination, and moonset were 1915 (May 17, 2000), 0026 (May 18, 2000), and 0502 (May 18, 2000), respectively. We measured the polarization of the moonlit night sky approximately in every half an hour after moonrise. Table 1 summarizes the recording data for the moonlit night sky.

Sunlight polarization measurements were carried out at different places and times in Finland (UTC+3; Sodankylä with pine forest type of area [*Gál et al.*, 2001a]) and Tunisia (UTC+1; Chott el Djerid with arid desert type of area [*Pomozi et al.*, 2001]). Although during our measuring campaign (from May 15 to 20, 2000, when the Moon was approximately full) we performed both daytime and nighttime celestial polarimetric measurements at the same site (Kunfehértó), the day sky was unfortunately always partly cloudy. Thus here we cannot present any pair of daytime/nighttime measurements of clear skies with approximately the same solar and lunar zenith angles at the same site. This is the reason why the clear-sky daytime measurements originate from other sites (Tunisia and Sodankylä).

Our Imaging Polarimetry Laboratory possesses a digital atlas of celestial polarization patterns measured by full-sky imaging polarimetry. From this atlas those polarization patterns of the sunlit clear sky were selected where the zenith angles θ_S of the Sun were approximately the same as the zenith angles θ_M of the full Moon in the moonlit night sky ($|\theta_M - \theta_S| \leq 2°$, Table 1 and Table 2). For the sake of an easier comparison, the polarization pattern of the sunlit sky with a given solar zenith angle was appropriately rotated until the solar azimuth angle coincided with the lunar azimuth angle in the corresponding polarization pattern of the moonlit night sky. This series of the polarization pattern of the clear sunlit day sky served as a control. Table 2 summarizes the recording data for the sunlit day sky.

2.2. Measurement of the Celestial Polarization Pattern by Full-Sky Imaging Polarimetry

Our full-sky imaging polarimetric technique used was similar to the method of *Voss and Liu* [1997]. An angle of view of 180° was ensured by a fisheye lens (Nikon-Nikkor, F-2.8, focal length: 8 mm) including a built-in rotating disc mounted with three neutral density linear polarization (type HNP'B) filters with three different polarization axes (0°, 45°, and 90° measured from the radius of the disc), and the detector was a photoemul-

Table 2. Recording Data of the Polarization Patterns of the Clear Sunlit Day Sky in Figures 2d-2f Measured by Full-Sky Imaging Polarimetry*

Row in Figures 2d-2f	Date 1999	Time UT	Place	Latitude, Longutude	Solar Zenith Angle θ_S	Exposure, s	Aperture
1, 2, 9	Aug. 26	0800	Chott el Djerid (Tunisia, UTC+1)	33°52'N, 8°22'E	69°	1/250	5.6
3, 7, 8	Aug. 26	1700	Chott el Djerid (Tunisia, UTC+1)	33°52'N, 8°22'E	66°	1/250	5.6
4, 5, 6	June 27	0900	Sodankylä (Finland, UTC+3)	67°25'N, 26°30'E	61°	1/60	8

*The solar azimuth angle φ was the same as the lunar azimuth angle in Table 1.

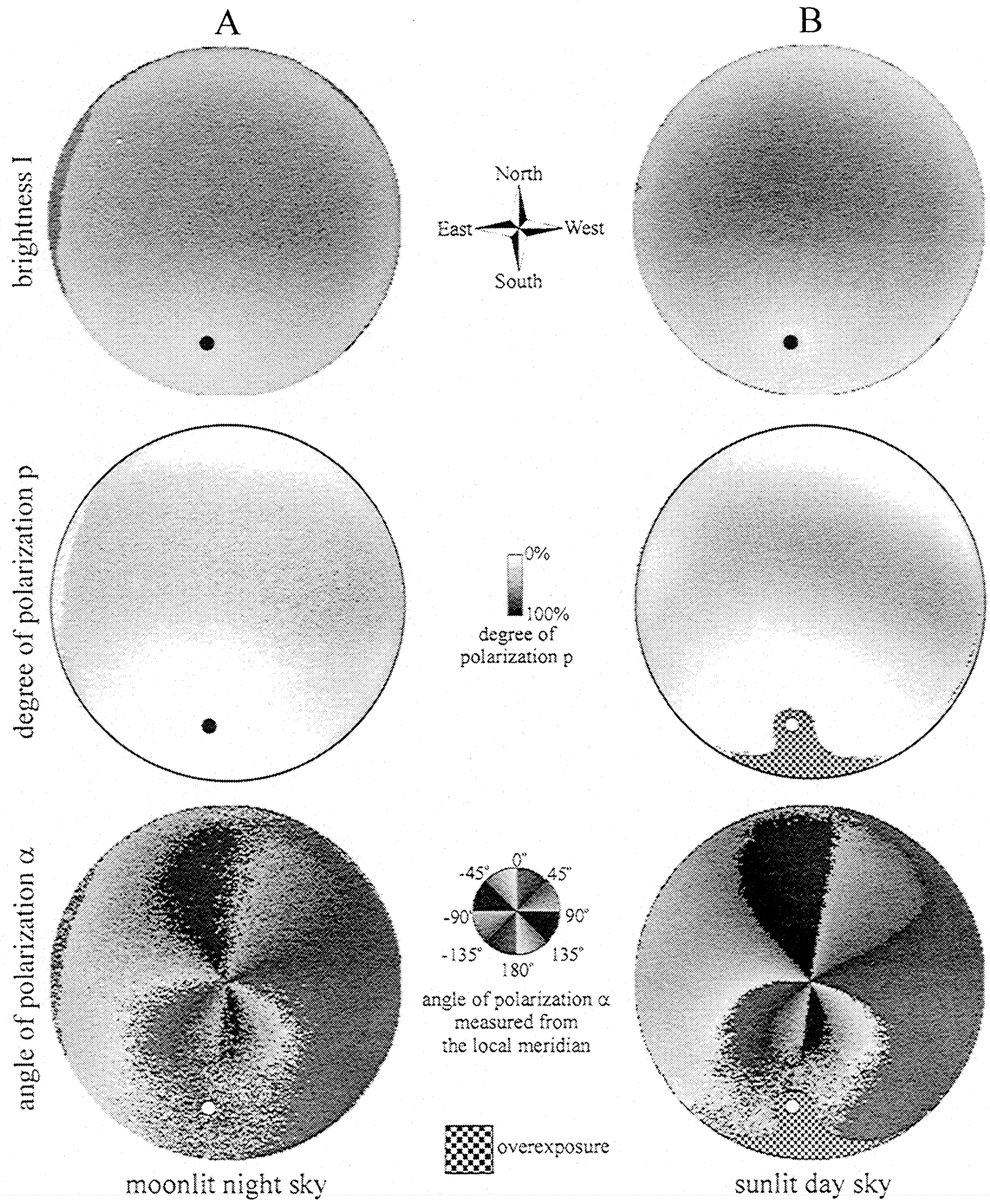

Figure 1. (a) Patterns of brightness I, degree of polarization p, and angle of polarization α (measured from the local meridian passing through the observed celestial point) of a particular clear moonlit night sky measured by full-sky imaging polarimetry in white light at lunar zenith angle of 63^o. (b) As for Figure 1a for a clear sunlit day sky in simulated white light at solar zenith angle of 61^o. These patterns and their recording data are the same as those in row 5 of Figure 2. The checkered regions in Figure 1b are overexposed. The positions of the Moon and Sun are indicated by black or white dots. East is on the left of the compass rose because we are looking up through the celestial dome rather than down onto a map. The insets show the gray codes of the numerical values of p and α. These patterns and their recording data are the same as those in row 5 of Figure 2.

sion in a photographic camera (Nikon F801). As detectors, we used Kodak Tmax P3200 (pushed up 6400 ASA) black and white photographic film for moonlight recordings (with an aperture of 2.8 and exposure of 15 s), and Fujichrome Sensia II 100 ASA color reversal film for sunlight recordings. The maxima and half band widths of the spectral sensitivity curves of the latter were $\lambda_{\text{red}} = 650 \pm 30$ nm, $\lambda_{\text{green}} = 550 \pm 30$ nm, $\lambda_{\text{blue}} = 450 \pm 50$ nm. From a given sky, three photographs were taken for the three different alignments of the transmission axis of the polarizers on the built-in rotating disc. Table 2 gives also the values of the

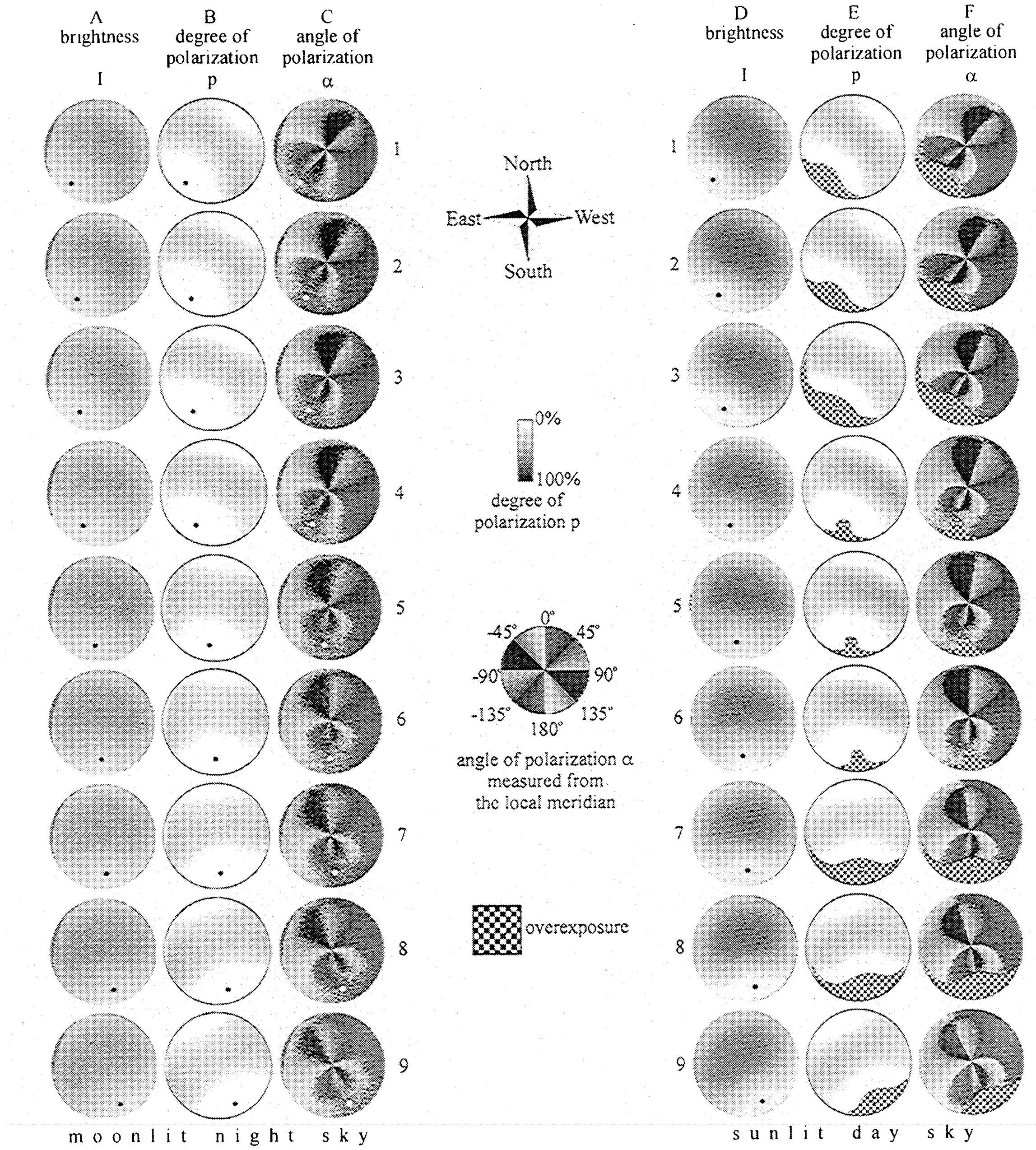

Figure 2. (a-c) Spatial distribution of brightness, degree, and angle of polarization over the entire clear moonlit night celestial hemisphere measured in white light for different zenith angles of the moon. (d-f) As Figures 2a-2c for the clear sunlit day sky measured in simulated white light for approximately the same zenith angles of the Sun as those of the Moon. Other conventions as in Figure 1.

exposure and aperture, with which the sunlit day sky was photographed. The camera was set up on a tripod in such a way that its axis passing through the view-finder pointed northward and the optical axis of the fisheye lens was vertical. Further details of our imaging polarimeter and its calibration were published by *Gál et al.* [2001a,2001b].

With the aid of a personal computer, the three developed pictures (black and white negative pictures of moonlit skies or color positive pictures of sunlit skies) belonging to a given sky were digitized in 3×8 bit (8 + 8 + 8: red + green + blue) with a Hewlett Packard ScanJet 6100C. The black and white negative pictures (I_-) of moonlit skies were transformed to black and white positive pictures (I_+) in such a way that the brightness value I_- of every pixel was set as $I_+ = 255 - I_-$, where 255 is the maximum of the digital brightness value. Then the patterns of the brightness, degree, and angle of polarization of skylight were determined and visualized as high-resolution color-coded two-dimensional circular maps. In the case of the sunlit day skies these patterns were obtained in the red, green, and blue spectral ranges, in which the three color-sensitive layers of the photoemulsion have the maximal sensitivity. Hence the red, green, and blue spectral ranges were obtained by using a digital image processing program provided

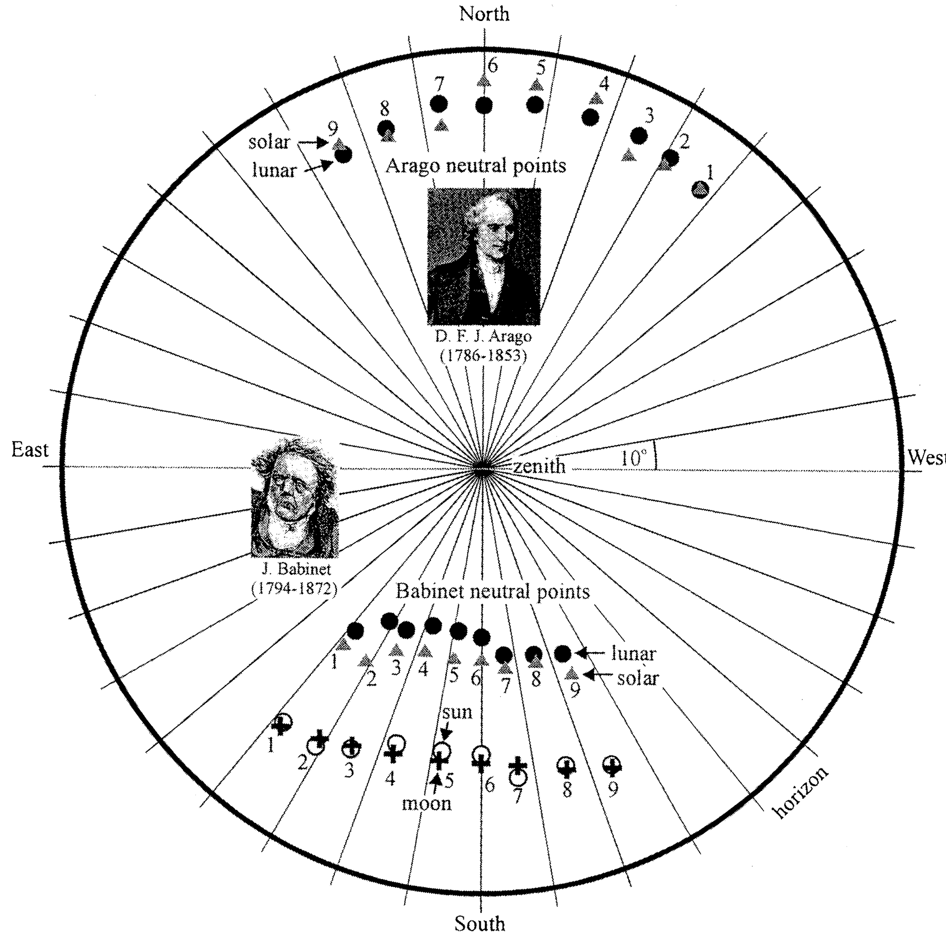

Figure 3. Positions of the Moon (crosses), Sun (circles), lunar (solid dots) and solar (shaded triangles) Arago and Babinet neutral points of the clear moonlit/sunlit night/day sky evaluated from the measured celestial polarization patterns in Figures 2b,2c/2e,2f. The numbers next to the dots/triangles correspond with the row numbers in Figure 2. The insets show the portraits of Dominique Francois Jean Arago and Jacques Babinet, who discovered the first (in 1810) and second (in 1840) neutral point of the sunlit day sky.

with the scanner to digitally separate the color channels in the digitized images. The computer evaluation of the three digitized photographs of a given sky, that is, the calculation of the brightness, degree, and angle of polarization, was practically the same as in the case of videopolarimetry [*Horváth and Varjú*, 1997].

In order to be able to compare the polarization of sunlit skies with that of the corresponding moonlit skies, the color pictures of the sunlit skies were transformed to averaged black and white pictures in the following way: The brightness value of every pixel of such a transformed black and white picture was set as $I_{average} = (I_{red}+I_{green}+I_{blue})/3$, where I_{red}, I_{green} and I_{blue} are the brightness values of the given pixel of the original color picture measured in the red, green, and blue spectral ranges, in which the three color-sensitive layers of the photoemulsion had the maximal sensitivity. This image processing procedure imitated well the white light sensitivity of the Kodak Tmax P3200 black and white film.

As the polarization of scattered sunlight [*Coulson*, 1988], also the polarization of scattered moonlight depends slightly on the wavelength [*Gehrels*, 1974]. This small wavelength dependency of the polarization patterns of the moonlit clear night sky was washed out by using black and white photographic film as detector: In order to minimize the time of exposure, the polarization characteristics of the moonlit sky must have been recorded by a highly sensitive photographic film. The most sensitive roll film available for us was Kodak Tmax P3200 black and white photoemulsion which could have been pushed up 6400 ASA. Using this film, a time of exposure of 15 s was needed at the maximal aperture of 2.8. Since this photographic film was black and white and because we could not use a color filter (that would have increased exposure time), we could measure the polarization of the scattered moonlight only in white light, that is, its brightness, degree, and angle of polarization was averaged by the photoemulsion over the full visible range (400–750 nm) of the spectrum.

The three-dimensional celestial hemisphere was represented in two dimensions by a polar coordinate system, where the zenith angle θ and the azimuth angle φ from north are measured radially and tangentially, respectively. In this two-dimensional coordinate system the zenith is at the origin and the horizon corresponds to the outermost circle.

3. Results and Discussion

Figure 1 shows the patterns of brightness, degree, and angle of polarization of a clear moonlit night sky with lunar zenith angle of 63^o and of a clear sunlit day sky with solar zenith angle of 61^o. Because of the rougher grain sturcture of the highly sensitive photoemulsion (Kodak Tmax P3200) used for moonlight measurements the patterns in Figure 1a are more noisy than those in Figure 1b. Figures 2a-2c show the spatial distribution of brightness, degree, and angle of polarization over the entire clear moonlit night sky measured in white light for different positions of the Moon. Figures 2d-2f represents the same patterns of the clear sunlit day sky measured in simulated white light for approximately the same positions of the Sun as those of the Moon in the night sky. In the checkered regions (in the immediate vicinity of the sun) of skies in Figures 1 and 2 the photoemulsion was overexposed and that resulted in unpolarized areas of the pictures after computer evaluation. In these regions of the sky the angle of polarization is undefined. Figures 1 and 2 show not significant differences between the measured polarization patterns of the moonlit and sunlit sky. The characteristics of the polarization pattern of the sunlit clear sky measured by imaging polarimetry for different solar zenith angles were analyzed and discussed by *Horváth et al.* [1998], *Horváth and Wehner* [1999], *Gál et al.* [2001a,2001b], and *Pomozi et al.* [2001].

On the angle of polarization maps in Figures 1 and 2, there is an 8-shaped region, the long axis of which is parallel to the lunar/solar and antilunar/antisolar meridians. The lunar/solar Arago and Babinet neutral points are positioned at the tips of this 8-shaped region where positive polarization (direction of polarization normal to the scattering plane, $\alpha = \pm 90^o$ with respect to the local meridian) switches to negative polarization (direction of polarization parallel to the scattering plane, $\alpha = 0^o, 180^o$). Figure 3 shows the positions of the Moon, Sun, lunar/solar Arago and Babinet neutral points of the clear moonlit/sunlit night/day sky evaluated from the celestial polarization patterns in Figures 2b, 2c/2e, and 2f. Table 3 summarizes the zenith angles of these lunar/solar Arago and Babinet neutral points of skylight polarization. The azimuth angles of the lunar/solar Arago or Babinet neutral points were the same as that of the antilunar/antisolar or lunar/solar meridian, respectively (due to the appropriate rotation of the patterns of the sunlit day sky).

Comparing the measured polarization patterns of the moonlit night sky (Figures 1a, 2b, and 2c) with that of the sunlit day sky (Figure 1b, 2e, and 2f), we can confirm that the polarization characteristics of a moonlit night sky are practically identical with that of a sunlit sky if the position of the Moon in the firmament is the same as that of the Sun. The small differences between the measured polarization patterns (Figures 1 and 2) and positions of the neutral points (Figure 3) of the moonlit clear night sky at full Moon and those of the sunlit clear day sky can be attributed to (in order of importance) (1) the probably different meteorological conditions (e.g., aerosol concentration) during the nighttime and daytime measurements, (2) the different local ground albedo at the places of measurement with different type of area, (3) the small differences ($|\theta_M - \theta_S| \leq 2^o$) between the solar and lunar zenith angles, (4) the different types of the detector (white light for moonlight, simulated white light for sunlight), (5) the slightly different polarization state of moonlight (being weakly linearly polarized [*Dollfus*, 1961; *Pellicori*, 1971]) and sunlight (being unpolarized), and (6) the different spectral features of moonlight (reflected from the Moon's surface) compared with sunlight [*Gehrels*, 1974]. The Monte Carlo method used by *Adams and Kattawar* [1997], for example, is able to model these differences for any input state of polarization.

We admit that these results are not surprising because they follow from the theory of light scattering: Considering the structure of the celestial polarization pattern, it is all the same if the Moon or the Sun is the light source. Nevertheless, also this must be experimentally proven, and the importance of our investigation is the presentation of the first comprehensive experimental evidence for this theoretical prediction.

In the future it would be interesting to study how the celestial polarization changes versus time after sunset (or prior to sunrise) if the Moon is visible in the sky. At full Moon, for the observer on the Earth's sur-

Table 3. Zenith Angles of the Lunar/Solar Arago and Babinet Neutral Points of Skylight Polarization Evaluated From the Celestial Polarization Patterns in Figures 2b,2c/2e. and 2f

	Row in Figure 2								
	1	2	3	4	5	6	7	8	9
Zenith angle of the lunar Arago point	76^o	78^o	79^o	79^o	79^o	78^o	79^o	76^o	74^o
Zenith angle of the solar Arago point	76^o	76^o	74^o	83^o	83^o	83^o	74^o	74^o	76^o
Zenith angle of the lunar Babinet point	44^o	38^o	38^o	35^o	35^o	36^o	40^o	41^o	43^o
Zenith angle of the solar Babinet point	48^o	48^o	43^o	41^o	41^o	41^o	43^o	43^o	48^o

face, the Moon is situated opposite the Sun (phase angle $\beta = 0^o$), and at new Moon it stays in the Sun's direction ($\beta = 180^o$). In the first or last quarter the phase angle is $\beta = 90^o$ or $\beta = 270^o$, respectively. After sunset (or prior to sunrise), there is an intermediate period when the contributions of scattered sunlight and moonlight to the celestial polarization pattern are roughly equal. At night, of course, the polarization of scattered moonlight dominates in the firmament. Using full-sky imaging polarimetry, one can study the transition of the polarization pattern of the sunlit day sky into the polarization pattern of the moonlit night sky. However, the Moon is 10 times weaker at first/last quarters than when it is full, and the transition from sunlit to moonlit sky is relatively narrow. Thus it is much harder to measure the skylight polarization at first/last quarter.

The results presented in this account may have functional significance for arthropod navigation. For example, *Kerfoot* [1967] reports that the foraging activities of nocturnal bees last as long as the Moon stays above the horizon. Furthermore, several insect and crustacean species have been shown to use the Moon as a navigational aid. However, as *Wehner* [1984] points out in reviewing these results, there is no unambiguous evidence that lunar time-compensated Moon compass orientation, analoguous to solar time-compensated Sun compass orientation, exists in any animal species.

Desert ants of the genus *Cataglyphis* are exclusively diurnal foragers, but when experimentally tested at night, they take the full Moon for the Sun and navigate according to what a solar time-compensated Sun compass would predict [*Wehner*, 1982]. However, what about nocturnal insects, i.e., species that usually forage at night? Even if they do not possess a lunar time-compensated Moon compass, they could use the Moon and the nighttime angle of polarization pattern described in this work as a short-term compass that is calibrated anew each time the animals start for a foraging journey [see, e.g., *Lambrinos et al.*, 1997]. The relatively low intensity of the polarized moonlit night sky may not be a limiting factor of the navigation by nocturnal insects because field crickets (*Gryllus campestris*), for instance, can respond to polarized light at intensities that are lower than under the clear, moonless night sky [*Herzmann and Labhart*, 1989].

Acknowledgments. This work was supported by a 3-year János Bolyai postdoctoral research fellowship received by G. Horváth from the Hungarian Academy of Sciences and by a 1-year doctoral research fellowship received by J. Gál from the George Soros Foundation (grant 230/2/878). Grant 31-43317.95 received by R. Wehner from the Swiss National Science Foundation is gratefully acknowledged. Many thanks are due to Balázs Bernáth and István Pomozi for their assistance during the moonlight and sunlight polarization measurements. We are grateful to three anonymous referees for their valuable comments on the manuscript.

References

Adams, J. T., and G. W. Kattawar, Neutral points in an atmosphere-ocean system, 1, Upwelling light field, *Appl. Opt., 36*, 1976-1986, 1997.

Coulson, K. L., *Polarization and Intensity of Light in the Atmosphere*, A. Deepak, Hampton, Va., 1988.

Dollfus, A., Polarization studies of planets, in *The Solar System*, edied by G. P. Kuiper, and B. M. Middlehurst, vol. 3, pp. 343-399, Univ. of Chicago Press, Chicago, Ill., 1961.

Gál, J., G. Horváth, V. B. Meyer-Rochow, and R. Wehner, Polarization patterns of the summer sky and its neutral points measured by full-sky imaging polarimetry in Finnish Lapland north of the Arctic Circle, *Proc. R. Soc. London, Ser. A, 457*, 1385-1399, 2001a.

Gál, J., G. Horváth, and V. B. Meyer-Rochow, Measurement of the reflection-polarization pattern of the flat water surface under a clear sky at sunset, *Remote Sens. Environ., 76*, 103-111, 2001b.

Gehrels, T. (Ed.), *Planets, Stars, and Nebulae Studied With Photopolarimetry*, Univ. of Ariz. Press, Tucson, 1974.

Herzmann, D., and T. Labhart, Spectral sensitivity and absolute threshold of polarization vision in crickets: A behavioral study, *J. Comp. Physiol. A, 165*, 315-319, 1989.

Horváth, G., J. Gál, I. Pomozi, and R. Wehner, Polarization portrait of the Arago point: Video-polarimetric imaging of the neutral points of skylight polarization, *Naturwissenschaften, 85*, 333-339, 1998.

Horváth, G., and D. Varjú, Polarization pattern of freshwater habitats recorded by video polarimetry in red, green and blue spectral ranges and its relevance for water detection by aquatic insects, *J. Exp. Biol., 200*, 1155-1163, 1997.

Horváth, G., and R. Wehner, Skylight polarization as perceived by desert ants and measured by video polarimetry, *J. Comp. Physiol. A, 184*, 1-7, 1999. (Erratum, *184*, 347-349, 1999.)

Kerfoot, W. B., The lunar periodicity of *Sphecodogastra texana*, a nocturnal bee (Hymenoptera: Halictidae), *Anim. Behav., 15*, 479-486, 1967.

Können, G. P., *Polarized Light in Nature*, Cambridge Univ. Press, New York, 1985.

Lambrinos, D., M. Maris, H. Kobayashi, T. Labhart, R. Pfeifer, and R. Wehner, An autonomous agent navigating with a polarized light compass, *Adapt. Behav., 6*, 131-161, 1997.

Pellicori, S. F., Polarizing properties of pulverized materials with special reference to the lunar surface, *Appl. Opt., 10*, 270-285, 1971.

Pomozi, I., G. Horváth, and R. Wehner, How the clear-sky angle of polarization pattern continues underneath clouds: full-sky measurements and implications for animal orientation. *J. Exp. Biol.*, in press, 2001.

Voss, K. J., and Y. Liu, Polarized radiance distribution measurements of skylight, I, System description and characterization, *Appl. Opt., 36*, 6083-6094, 1997.

Wehner, R., Himmelsnavigation bei Insekten. Neurophysiologie und Verhalten, *Neujahrsbl. Naturforsch. Ges. Zürich, 184*, 1-132, 1982.

Wehner, R., Astronavigation in insects, *Annu. Rev. Entomol., 29*, 277-298, 1984.

Wolstencroft, R. D., and J. C. Brandt, Multicolor polarimetry of the night sky, in *Planets, Stars, and Nebulae Studied With Photopolarimetry*, edited by T. Gehrels, pp. 768-780, Univ. of Ariz. Press, Tucson, 1974.

A. Barta, J. Gál, G. Horváth, Department of Biological Physics, Eötvös University, Pázmány sétány 1., H-1117 Budapest, Hungary (gh@arago.elte.hu)

R. Wehner, Zoologisches Institut, Universität Zürich, Winterthurerstrasse 190, CH-8057 Zürich, Switzerland

(Received October 18, 2000; revised May 1, 2001; accepted May 21, 2001.)